AIAA 2000-1385

BI-STABLE COMPOSITE SHELLS

K. Iqbal* **and S. Pellegrino†**

Department of Engineering, University of Cambridge,
Trumpington Street, Cambridge, CB2 1PZ, U.K.

Abstract

This paper is concerned with a new type of deployable structures that can be rolled up like a tape measure but, unlike a tape measure, are *stable* in two different configurations. The key to the behaviour of these structures is a particular type of composite construction based on an anti-symmetric lay-up of glass fibres in a polypropylene matrix. The paper presents a finite element analysis using the ABAQUS package of the process of rolling up a bi-stable cylindrical shell. The results of this simulation provide considerable new insights into the structural mechanics of bi-stable shells, as well as predicting the stress distribution, curvature variation, etc. in the rolled-up shell.

Introduction

This paper investigates a type of shell structures that can be rolled up like a standard steel tape measure but, unlike a tape measure, are *stable* in two different configurations, as shown in Fig. 1.

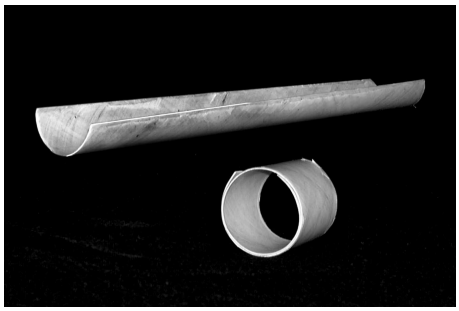

Figure 1: Extended and rolled-up configurations of a bi-stable composite shell.

Our interest in this type of structures arises from their potential applications in the field of deployable structures. One such application, extendible booms, is illustrated in Figure 2. This photograph shows a boom that is used as a telescopic camera mount for the inspection of nuclear power stations; its extended length is over 10 m with a diameter of about 200 mm. Note that the containment structure "around" the boom is absolutely minimal, which is in great contrast with the deployment cassette of a standard bi-STEM boom, with diameter around 25 mm, shown in Figure 3.

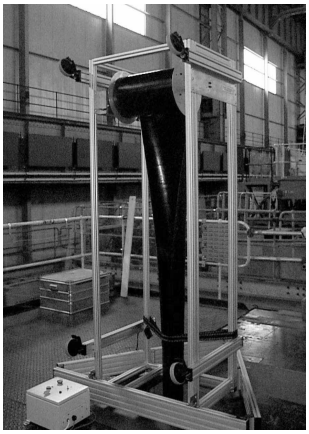

Figure 2: Telescopic camera mount based on bi-stable tube (Courtesy of Rolatube Ltd).

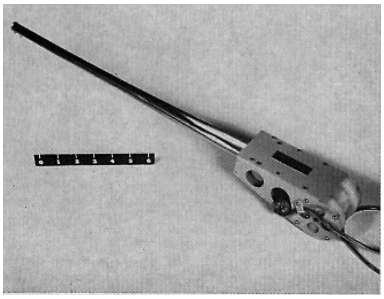

Figure 3: Bi-STEM boom (Rimrott, 1965).

Normally, a cylindrical shell structure that has been flattened and rolled up, as shown in the examples above,

*Research Student.
†Reader in Structural Engineering, Associate Fellow AIAA.

is in a high-energy, unstable state. Therefore a containment/deployment mechanism is required to prevent the structure from releasing its stored elastic energy in an uncontrolled way. By using bi-stable shell structures we can avoid, or much reduce the need for a deployment mechanism.

The shell shown in Fig. 1 is strain free in the straight, extended configuration, but is subject to high levels of strain in the second, rolled-up configuration. However, it is unable to jump from the second configuration to the first without a substantial energy input because the rolled-up configuration corresponds to a local minimum for the potential energy surface of the structure.

The layout of this paper is as follows. The next section gives a brief history of the development of bi-stable composite structures and relates their behaviour to the way they are constructed. A simple analytical method, previously developed, is briefly outlined. The following section describes the simulation techniques that have been developed to study the behaviour of bi-stable shells. They are validated against experimental data from a tension test and a bending test on flat plates. New insights are gained into the non-linear behaviour observed in the bending test. Next, the simulation of the process of rolling up a cylindrical shell —and leaving it rolled up when all external loads are removed— is described. Results that are obtained from this simulation include the stress distribution in the coiled-up shell, its longitudinal radius of curvature, and the profile of the transverse cross-sections. A comparison between the results from the finite element simulation, the simple analytical model, and experimental measurements concludes the paper.

Background

Bi-stable composite shells were discovered by Daton-Lovett (1996). The inventor visited the Deployable Structures Laboratory, in Cambridge, in the summer 1996 and showed us several of his models. That visit signalled the beginning of a continuing collaboration with Daton-Lovett. During the last three years we have carried out a number of studies with the aim of developing a better understanding of the structural mechanics of these structures, as well as analytical and computational models to predict their behaviour.

In a previous paper (Iqbal et al. 1998) we have presented a simple analytical model that captures the key features of bi-stable cylindrical shells. Because that paper provides the background for the present numerical study, in this section we summarize its main findings.

The bi-stable behaviour of cylindrical shell structures originates from the fact that the transformation of a surface of zero gaussian curvature (recall that the gaussian curvature is the product of the two principal curvatures) into other surfaces of zero gaussian curvature requires only bending energy, as the transformation of the mid-surfaces is isometric. By arranging stiff fibres in a suitable lay-up, one can create preferential directions of bending for the shell and thus, when the shell is deformed by a sufficiently large amount from its original, unstressed configuration, it will "flip" into an alternative configuration with zero gaussian curvature.

To avoid that the shell ends up in a twisted configuration when it flips, Daton-Lovett chose to use an anti-symmetric lay-up, thus almost eliminating coupling between bending and twisting. This makes it possible to compactly roll-up a cylindrical shell.

Analytically, this can be seen in the $\mathbf{ABD}$ matrix (Hyer, 1998) relating the mid-surface strains and curvatures to the corresponding stress resultants in the shell

$$\begin{bmatrix} N_x \\ N_y \\ N_{xy} \\ M_x \\ M_y \\ M_{xy} \end{bmatrix} = \begin{bmatrix} \mathbf{A} & \mathbf{B} \\ \mathbf{B} & \mathbf{D} \end{bmatrix} \begin{bmatrix} \epsilon_x \\ \epsilon_y \\ \gamma_{xy} \\ \kappa_x \\ \kappa_y \\ \kappa_{xy} \end{bmatrix} \tag{1}$$

Table 1: Properties of PP/Glass unidirectional lamina.

Young's Modulus along the fibres	26.6 GPa
Young's Modulus across the fibres	2.97 GPa
Shear Modulus	1.39 GPa
Major Poisson's ratio	0.4
Minor Poisson's ratio	0.04

Taking the x and y-axes to coincide with the longitudinal and transverse directions of the shell, as shown in Fig. 4(a), for a 5-ply laminate [+45/-45/0/+45/-45] with the unidirectional properties listed in Table 1 the $\mathbf{ABD}$ matrix is

$$\left[\begin{array}{ccc|ccc} 13.9 & 6.0 & 0 & 0 & 0 & -0.55 \\ 6.0 & 8.8 & 0 & 0 & 0 & -0.55 \\ 0 & 0 & 6.19 & -0.55 & -0.55 & 0 \\ \hline 0 & 0 & -0.55 & 0.97 & 0.67 & 0 \\ 0 & 0 & -0.55 & 0.67 & 0.95 & 0 \\ -0.55 & -0.55 & 0 & 0 & 0 & 0.69 \end{array}\right] \tag{2}$$

here the units are GPa mm for $\mathbf{A}$, GPa mm^2 for $\mathbf{B}$, and GPa mm^3 for $\mathbf{D}$. From now on, the ply angle will be denoted by α.

Because the coefficients D_{13} and D_{23} are zero, bending and twisting are now decoupled. Therefore, the longitudinal and transverse directions of curvature of the tube will be principal directions of curvature also in the rolled-up configuration, and hence each turn will overlap the previous, as it is clearly the case in Fig. 2. Also note that $\mathbf{B} \neq 0$ for the anti-symmetric laminate, but the resulting coupling between bending and stretching behaviour has only a weak effect on the bi-stability of the shell.

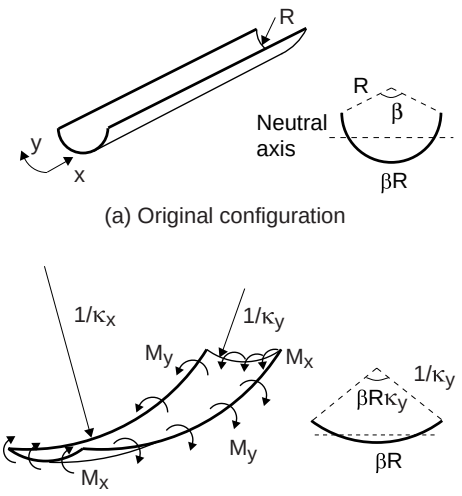

(a) Original configuration

(b) Deformed configuration

Figure 4: Uniform bending of cylindrical shell.

A simple model for the bi-stability of a shell structure with uniform transverse curvature, $1/R$, that is subjected to uniform curvature changes κ_x and $\kappa_y - 1/R$, Fig. 4, was proposed by Iqbal et al. (1998).

The strain energy in the shell has the expression

$$U = U_b + U_s \tag{3}$$

where the bending and stretching energies have the following approximate expressions

$$\begin{aligned} U_b &= \frac{1}{2}\beta R[D_{11}\kappa_x^2 + 2D_{12}\kappa_x(\kappa_y - \frac{1}{R}) \\ &\quad + D_{22}(\kappa_y - \frac{1}{R})^2] \qquad (4) \\ U_s &= \frac{A_{11}}{2}[\frac{\beta R}{2}\frac{\kappa_x^2}{\kappa_y^2} + \frac{\sin(\beta R\kappa_y)}{2}\frac{\kappa_x^2}{\kappa_y^3} \\ &\quad - \frac{4\sin^2(\beta R\kappa_y/2)}{\beta R}\frac{\kappa_x^2}{\kappa_y^4}] \qquad (5) \end{aligned}$$

Figure 5 shows a contour plot of the total strain energy for a shell with $\alpha = 45^\circ$ as a function of the total curvatures in the longitudinal and transverse directions, κ_x vs. κ_y. The transverse radius of the shell is $R = 25$ mm, and the angle subtended by the cross section is $\beta = 160^\circ$.

As well as having an absolute minimum ($U = 0$) at $\kappa_x = 0$, $\kappa_y = 1/R = 0.04$ mm^{-1}, which be readily verified on the left-hand side inset plot (U vs. κ_y), the plot shows the existence of a local minimum at $\kappa_y \approx 0$ and $\kappa_x \approx 1/36$ mm^{-1}. This local minimum corresponds to the rolled-up configuration of the shell.

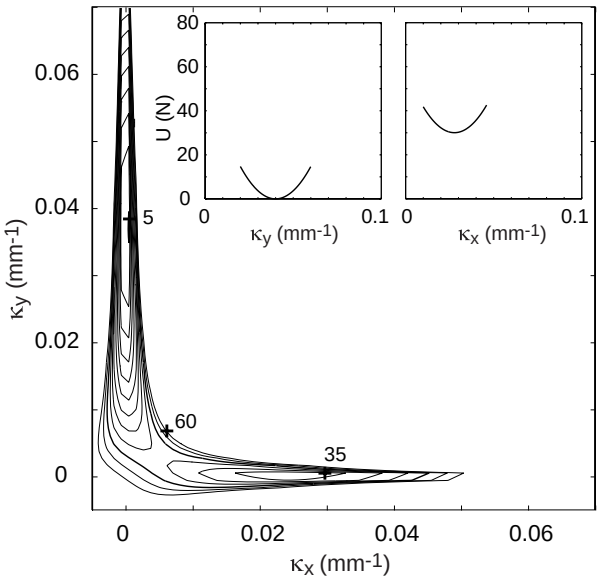

Figure 5: Energy plot for shell with $\alpha = 45^\circ$ and $R = 25$ mm.

This simple model is able to capture the main features of the folding of cylindrical bi-stable shells. However, it is of limited accuracy in predicting the value of the coiled-up radius of the shell: it typically overestimated R by about 20% for $\alpha = 45^\circ$ and by up to 50% for larger values of α. Also, because the model assumes uniform curvature changes, it cannot provide accurate estimates of the peak strain that occurs during coiling; knowing this value is important for design purposes.

Finite Element Modelling

An extensive computational study of bi-stable composite shells was carried out using the finite-element package ABAQUS (Hibbitt et al.,1999). Initially, thin shell elements S8R5 (8 nodes, reduced integration, 5 degrees of freedom per node) were used with the *composite* option to create five layers within the thickness of the shell element. In each layer, of specified thickness, the direction of the fibres was defined by the *orientation* command. This creates a local co-ordinate system for each layer, which in a large displacement analysis rotates with the average rigid body motion of the material point.

The thin shell elements worked well for the moderately non-linear analyses that were carried out at the beginning and which are described next. However, general purpose shell elements, such as S4R (4 nodes, reduced integration), were found to have more robust convergence properties in the heavily non-linear simulations that are described in the section Simulation of Bi-stable Shells.

Linear-elastic behaviour was assumed for each lamina, the material properties being those listed in Table 1.

Validation of FE model

The accuracy of the model was tested by simulating the behaviour of a flat composite plate with the same anti-symmetric lay-up of the bi-stable shell. Flat plates had previously been tested experimentally, in tension and in bending. Their mid-plane strains and the curvatures at the centre of the plate had been estimated from surface-mounted strain gauge measurements.

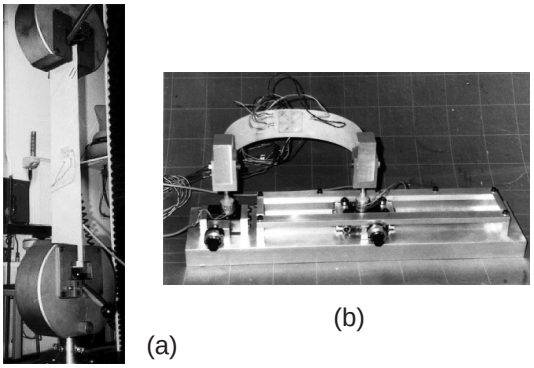

Figure 6: Tension and bending tests on composite plates.

The tension test, Fig. 6(a), had been performed with a standard Instron materials testing machine on a 535 mm $\times$ 102 mm plate with a thickness of 1.03 mm. Due to its anti-symmetric lay-up, the plate was not flat — this is due the effect of unbalanced stresses during cooling, see Hyer (1981). It was found that including this out-of-flatness in the FE model was essential to correctly capture the relationship between the axial stress resultant, N_x, and the mid-plane strains. The results are shown in Fig. 7.

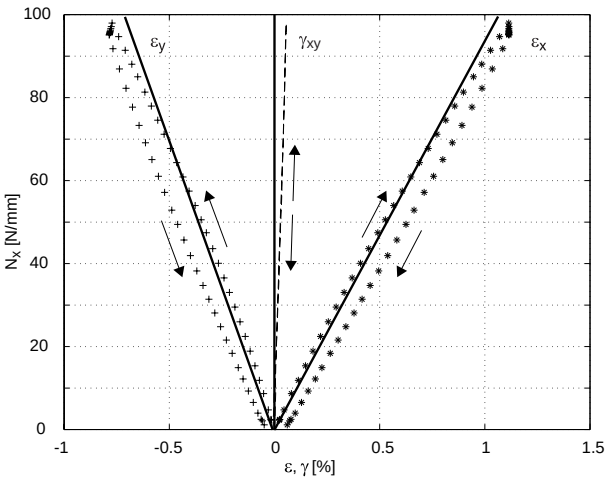

Figure 7: Experimental measurements and FE predictions for tension test.

The experiment had been carried out at a strain rate of 3×10^{-4} s^{-1}; the figure clearly shows some creep effects. At higher strain rates creep effects become smaller, but some non-linearity in the elastic behaviour of the material remains. This has not been accounted for in our present FE work.

The solid lines in Fig. 7 correspond to the FE simulation results obtained from a mesh of 200 $\times$ 8 S8R5 elements. The run options were *static, non-linear geometry*, but in fact there is hardly any non-linear behaviour. The initial twist of the plate was simulated by seeding an out-of-plane imperfection of sinusoidal shape. The maximum amplitude was 5 mm at the quarter points, along the edges of the plate.

The bending test required the use of a special apparatus, as a standard four-point-bending arrangement had been found unsuitable to test a plate that undergoes large changes of curvature. Therefore, a bending machine was used that imposes equal rotations to end blocks attached to the specimen, while measuring the required end torques. One of the end blocks is mounted on a linear bearing, to eliminate any longitudinal constraint on the specimen.

A 252 mm long by 40 mm wide plate was tested, and the results are reported in Fig. 8. In marked contrast with the behaviour in tension, the bending test showed a considerable amount of geometric non-linearity, mainly associated with the transverse curvature κ_y. A simulation of this test, using a mesh of 200 $\times$ 8 S8R5 elements with a 2 mm twisting imperfection as in the previous analysis (run options: static, non-linear geometry, Riks) was able to explain this behaviour.

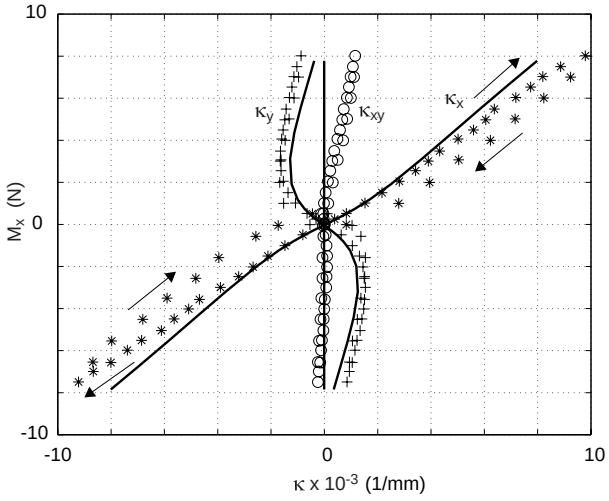

Figure 8: Experimental measurements and FE predictions for bending test.

For small applied moments M_x the transverse deformation of the plate is fairly uniform, as in a standard isotropic plate. As M_x increases in magnitude, the central part of the plate becomes approximately flat and then proceeds to reverse its curvature, see the sequence of cross-sections

plotted in Fig. 9. This causes the plate to become longitudinally stiffer, to a small extent.

It is remarkable that, having properly modelled this effect, the FE simulation of the bending and twisting curvatures at the centre of the plate are in excellent agreement with the values measured in the experiment, Fig. 8. As in the tension test, creep effects are still not accounted for.

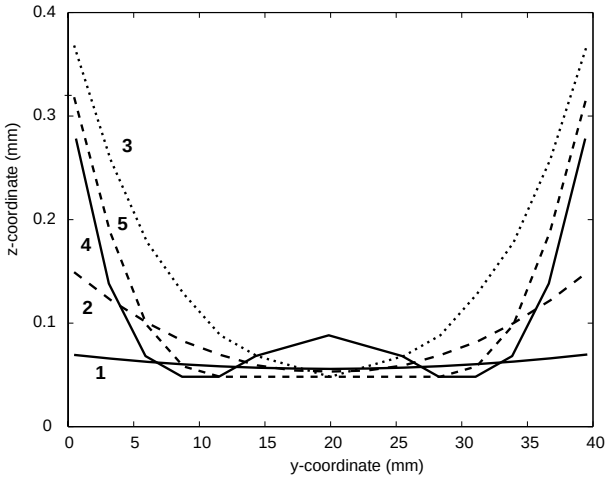

Figure 9: Deformation of central cross-section during bending test; 1 to 5 denote increasing bending moments.

Simulation of Bi-stable Shells

Most of the results presented in this section were obtained by analysing a cylindrical shell with five-ply anti-symmetric lay-up ($\alpha = 45°$). The geometric properties of the shell are as follows: mid-plane transverse radius $R = 25$ mm, angle of embrace $\beta = 180°$, length $L = 90$, thickness $t = 1.1$ mm

The shell was modelled by a mesh of 25 by 25 general-purpose S4R shell elements, which were found to be the most robust for this type of analysis. Different values of L and β, as well as different mesh densities and element types were investigated; further information is given at the end of this section.

The following three issues had to be resolved before a satisfactory simulation of the bi-stability of the shell could be obtained: how to drive the simulation, boundary conditions, choice of solution method.

On the first issue, attempts were first made to drive the change of configuration by imposing edge rotations along the initially straight edges of the shell. This seemed the obvious way of proceeding, based on the standard practice of using nodal displacements or rotations as control parameters in the analysis of structures that exhibit snapping. The problem with imposing edge rotations in the present case is that they are about fixed axes, which is incompatible with the large rotations that occur during rolling-up of the shell. It was found that applying edge moments using the *follower* option worked much better.

Regarding the choice of suitable boundary conditions, the point to note is that —due to the anti-symmetric lay-up of the shell— there is a small degree of asymmetry in the structure; hence symmetry considerations are not applicable. Therefore, the whole shell was analysed, and only a single node was restrained, in all six degrees of freedom. No stress concentrations arise at this node, because the loads applied to the shell are self-equilibrated. The particular node that was constrained was the node right at the centre of the mesh but, of course, any other node could have been chosen.

On the third issue, the arc-length solution method available in ABAQUS did not work well, despite several attempts to try different step size and convergence parameters. Instead, the automatic stabilization that has become available in recent versions of ABAQUS was successfully used. This method carries out a pseudo-dynamic simulation as soon as a negative pivot is detected during the inversion of the stiffness matrix. Thus, the algorithm is able to cope with localized snaps that occur in the mesh. Fictitious nodal masses and a small amount of numerical damping are introduced by ABAQUS to stabilize the snap.

The maximum value of the edge moment that was assigned is greater than the moment required to flatten the shell. This value can be estimated by substituting $M_x = 0$ and $\kappa_y = -1/R$ in Equation 1 and solving for the corresponding values of κ_x and M_y. In fact, the shell becomes unstable before this value is reached and ABAQUS starts to track down the motion of the shell as it snaps. The progress of this computation was monitored visually and, once the rolled-up configuration had clearly set in, the current run was halted. At this point, the edge moments were removed by running a new load step, with the option *op=new*. It has been found that it is best to avoid using the stabilise option during unloading, as it leads to inaccuracies in the final, fully unloaded configuration.

Figure 10 shows a complete simulation of the process of rolling-up the shell; the corresponding load-displacement history is shown in Fig. 11. The shell is initially unloaded, Fig. 10(a), and its response is linear until the shell becomes almost completely flat. In the configuration of Fig. 10(b), see also point b in Fig. 11, the follower moment starts to decrease as snapping begins. Here the shell begins to roll up and continues to do so until, see the configuration in Fig. 10(e), the current load step is terminated. At this point a new load step was executed to remove the edge moments, which produced the final configuration shown in Fig. 10(f).

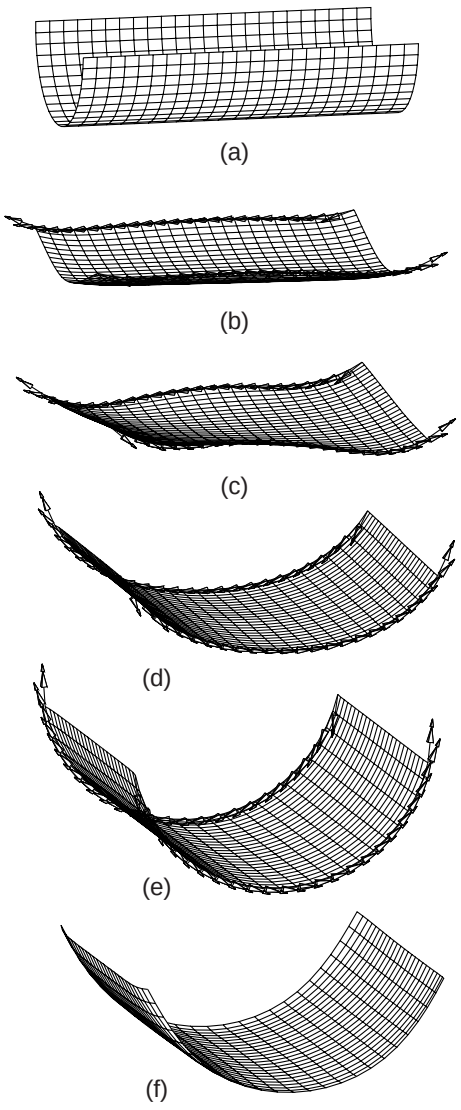

Figure 10: Finite-element simulation of a bi-stable shell.

The edge moments can be removed earlier than in this particular run: provided that the coiled-up configuration has developed sufficiently, the shell will remain "captured" in this configuration.

The results of this and other simulations of this kind have been particularly useful in gaining a detailed insight into the local deformation of the shell, from which the underlying structural mechanics of bi-stable shells can be understood. It is particularly interesting to look at the distribution of longitudinal stresses in the mid-plane of the shell, in the coiled configuration. Although all the external loads have now been removed, the shell is subject to high stress levels near the longitudinal edges: the peaks are -129 MPa right along the edges and $+45$ MPa in narrow regions that run longitudinally a small distance into the shell.

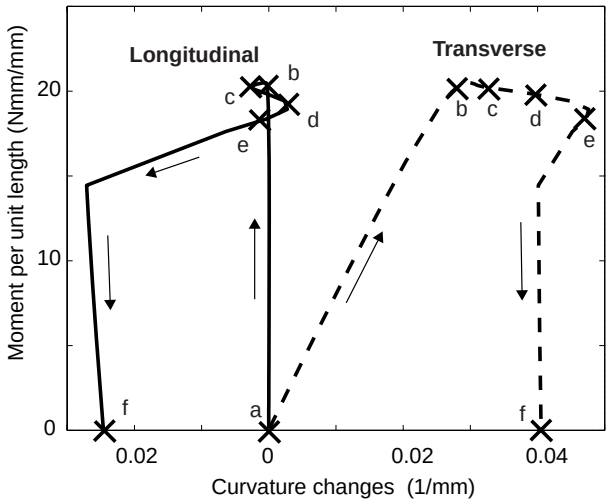

Figure 11: Applied moment vs. curvature changes at the centre of the shell.

It is also interesting to observe that the transverse bending moment in the rolled-up configuration is not zero, otherwise the transverse cross-section of the shell would still have the original curvature, but must be zero right at the edge. Hence two curved "lips" form near the edges, as the bending moment gradually builds up to the value required to bring the transverse curvature to zero. These "lips" can be seen, just, in Fig. 10(f).

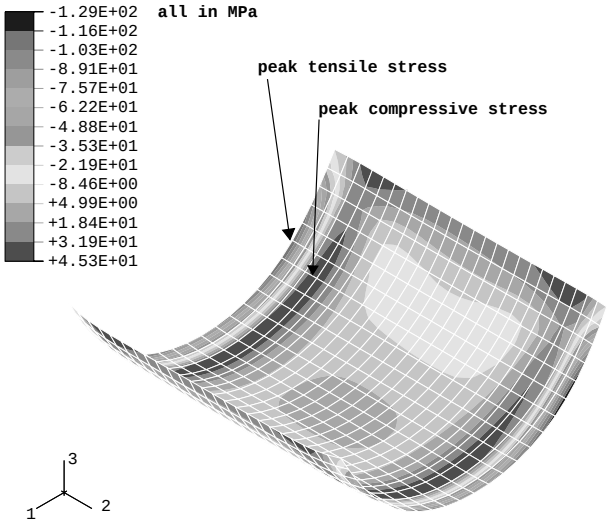

Figure 12: Longitudinal stress in coiled configuration.

In concluding, it is noted that the results presented in this section have been confirmed by running the same analysis with other types of elements. Convergence to approximately the same results was obtained with the elements S4 and S8R; the thin shell elements S4R5 and S8R5 were also tried, but the analysis could not be completed.

Computation of average curvatures

We are interested in computing from the FE simulation results the radius of coiling of the shell, as well as the shape of its transverse cross-sections. To do this, the final coordinates of a set of nodes lying on a section through a point q need to be transformed to the local coordinate system t_1, t_2, n defined in Fig. 13.

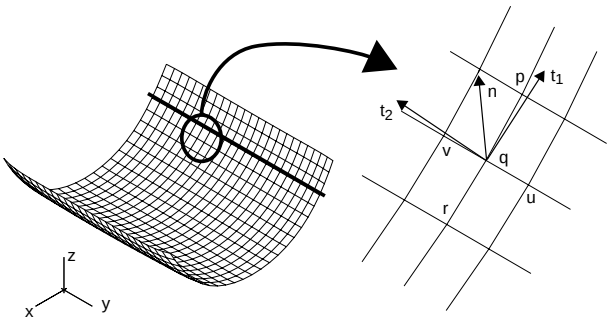

Figure 13: Node numbering for curvature computation .

The transformation matrices are

$$R_\alpha = \begin{bmatrix} \cos\alpha & 0 & \sin\alpha \\ 0 & 1 & 0 \\ -\sin\alpha & 0 & \cos\alpha \end{bmatrix} \quad (6)$$

$$R_\gamma = \begin{bmatrix} 1 & 0 & 1 \\ 0 & \cos\gamma & \sin\gamma \\ 0 & -\sin\gamma & \cos\gamma \end{bmatrix} \quad (7)$$

$$R_\beta = \begin{bmatrix} \cos\beta & sin\beta & 0 \\ -\sin\beta & \cos\beta & 0 \\ 0 & 0 & 1 \end{bmatrix} \quad (8)$$

where the rotations have the following expressions in terms of the global coordinates of the four points nearest to point q

$$\alpha = \tan^{-1}\Big(\frac{r_k - p_k}{p_i - r_i}\Big)$$
$$\gamma = \tan^{-1}\Big(\frac{v_k - u_k}{v_j - u_j}\Big)$$
$$\beta = \tan^{-1}\Big(\frac{v_i - u_i}{v_j - u_j}\Big)$$

Hence, the local coordinates of an arbitrary node are

$$\begin{bmatrix} x' \\ y' \\ z' \end{bmatrix} = R_\gamma R_\beta R_\alpha \begin{bmatrix} x \\ y \\ z \end{bmatrix} \quad (9)$$

The local coordinates obtained thus have been used to estimate the best fit circle through a whole section of the shell, etc. using Matlab (MathWorks, 1999).

Edge Deformation

Our finite-element simulation of the bi-stability of the shell has shown that two curved "lips" form near the edges of the shell, in the coiled-up configuration. The formation of these lips is associated with the linear-elastic unloading of the coiled-up shell from point e to point f in Figure 11. Once the configuration of Fig. 10(e) has been reached — note that there are no lips in this configuration— removal of the edge moments is equivalent, of course, to applying a set of equal and opposite moments on the shell.

The response to this loading system is a small displacement problem, and we can obtain an approximate answer using standard shell theory. Calladine (1983) gives the following expression for the edge deformation of an *isotropic, semi-infinite, closed cylindrical shell* subjected to bending moments M_x per unit length on its free edge:

$$w = -\sqrt{2} m e^{-\xi} \sin(\xi + \delta) \quad (10)$$

where

$$m = \frac{\mu^2 M_x}{2D}, \quad \mu = \frac{\sqrt{rt}}{\sqrt[4]{3(1-\nu^2)}}, \quad \text{and } \xi = \frac{x}{\mu}$$

This formula can be applied to anisotropic shells by calculating m and μ from

$$m = \frac{\mu^2 M_x}{2D_{11}}, \quad \mu = \sqrt{r}\sqrt[4]{4 d_{11} A^*_{22}}$$

where A^*_{ij} are the coefficients of $\mathbf{A}^{-1}$ and $\mathbf{d}_{ij}$ is the partially inverted stiffness matrix

$$\mathbf{d} = \mathbf{D} - \mathbf{B}\mathbf{A}^{-1}\mathbf{B} \quad (11)$$

A, **B** and **D** are the membrane, coupling and bending stiffness matrices, respectively, first introduced in Equation 1.

The same analysis has been carried out using ABAQUS, but this time for an open shell with transverse radius equal to the radius of coiling of the shell, as a *geometrically linear analysis*. The results of the above two calculations are plotted in Fig. 14, together with the cross-sectional shape predicted by the whole non-linear ABAQUS simulation of the coiling process.

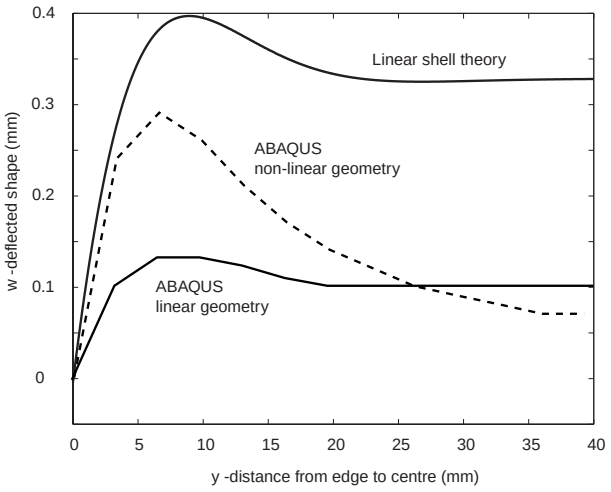

Figure 14: Edge deformations of a bi-stable shell.

It is found that the different predictions of the lip in the rolled-up shell have approximately the same shape, but the deflection amplitudes from the two linear approaches differ significantly between one another, and from the non-linear prediction.

Discussion

The results from the FE simulation carried out in the present study are compared to the simple analytical model in Iqbal et al. (1998) and to a set of experimental measurements in Table 2. In the table, r_e, r_a, r_f are the coiled-up radii obtained from the experiments, the analytical model and the present finite-element simulations, respectively.

Table 2: Comparison of rolled-up radii (mm).

α	R	L	β	r_e	r_a	r_f
$45°$	29	200	$280°$	30	42	42
$45°$	29	200	$200°$	30	42	44
$45°$	29	200	$120°$	32	44	49
$45°$	29	200	$90°$	33	45	55
$60°$	29	150	$280°$	13	26	28
$60°$	29	150	$200°$	13	27	30
$60°$	29	90	$120°$	14	28	33
$60°$	29	90	$70°$	15	33	38

For the case $\alpha = 45°$, note that the coiled radii predicted from the analytical model and the FE simulation are remarkably close for shells that subtend angles $\beta = 280°, 200°$ but differ by up to 25% for angles of $120°$ or less. The experimentally measured radii are 30% to 40% smaller for $\alpha = 45°$ and 55% to 75% smaller for $\alpha = 60°$.

It is believed that the main source of these discrepancies is in the non-linear behaviour of the material. Further work on this is currently under way.

Acknowledgments

We are grateful to Mr A. Daton-Lavett and Dr S.D. Guest for helpful discussions and to Rolatube Ltd for assistance with the experimental work.

References

Calladine, C. R. (1983). Theory of Shell Structures. *Cambridge University Press*, Cambridge.

Daton-Lovett, A. (1996). An extendible member. *Patent Cooperation Treaty Application*, PCT/GB97/00839.

Hibbitt, Karlsson and Sorenson Inc. (1999), *ABAQUS Users' Manual*, Version 5.8.

Hyer, M. W. (1981) Some observations on the cured shape of thin unsymmetric laminates. *Journal of Composite Materials* **15**, pp. 175-194.

Hyer, M. W. (1998) Stress Analysis of Fiber-Reinforced Composite Materials. *WCB/McGraw-Hill*, Boston.

Iqbal, K., Pellegrino, S. and Daton-Lovett, A. (1998). Bistable composite slit tubes. In: *Proc. IUTAM-IASS Symposium on Deployable Structures*, 6-9 September 1998, Cambridge.

MathWorks, Inc. (1999), *Matlab Users' Manual*, Version 5.3.